AD-A087 896 IOWA UNIV IOWA CITY DEPT OF PHYSICS AND ASTRONOMY F/G 3/2
SATELLITE SWEEPING OF ELECTRONS AND PROTONS IN SATURN'S INNER M--ETC(U)
JUL 80 R RAIRDEN N00014-76-C-0016
UNCLASSIFIED U. OF IOWA-80-29 NL

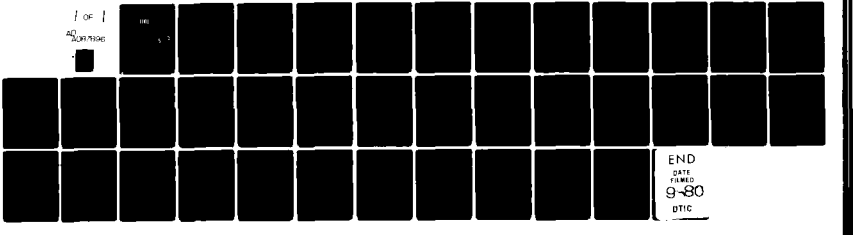

12

U. of Iowa 80-29

LEVEL II

SATELLITE SWEEPING OF ELECTRONS AND PROTONS IN SATURN'S INNER MAGNETOSPHERE

by

R. Rairden

Department of Physics and Astronomy
The University of Iowa
Iowa City, Iowa 52242

July 1980

UNCLASSIFIED

SECURITY CLASSIFICATION OF THIS PAGE (When Data Entered)

REPORT DOCUMENTATION PAGE

READ INSTRUCTIONS BEFORE COMPLETING FORM

1. REPORT NUMBER: U. of Iowa-80-29	2. GOVT ACCESSION NO.: AD-A087896
3. RECIPIENT'S CATALOG NUMBER: --	
4. TITLE (and Subtitle): SATELLITE SWEEPING OF ELECTRONS AND PROTONS IN SATURN'S INNER MAGNETOSPHERE	5. TYPE OF REPORT & PERIOD COVERED: Progress, ~~July~~ 1980
	6. PERFORMING ORG. REPORT NUMBER: --
7. AUTHOR(s): R. Rairden	8. CONTRACT OR GRANT NUMBER(s): N00014-76-C-0016
9. PERFORMING ORGANIZATION NAME AND ADDRESS: Department of Physics and Astronomy, The University of Iowa, Iowa City, Iowa 52242	10. PROGRAM ELEMENT, PROJECT, TASK AREA & WORK UNIT NUMBERS: --
11. CONTROLLING OFFICE NAME AND ADDRESS: Office of Naval Research, Electronics Program Office, Arlington, Virginia 22217	12. REPORT DATE: Jul~~y~~ 1980
	13. NUMBER OF PAGES: 36
14. MONITORING AGENCY NAME & ADDRESS (if different from Controlling Office)	15. SECURITY CLASS. (of this report): UNCLASSIFIED
	15a. DECLASSIFICATION/DOWNGRADING SCHEDULE

16. DISTRIBUTION STATEMENT (of this Report)

Approved for public release; distribution unlimited.

17. DISTRIBUTION STATEMENT (of the abstract entered in Block 20, if different from Report)

18. SUPPLEMENTARY NOTES

19. KEY WORDS (Continue on reverse side if necessary and identify by block number)

Satellites of Saturn
Saturn's Magnetosphere

20. ABSTRACT (Continue on reverse side if necessary and identify by block number)

[See page following.]

DD FORM 1 JAN 73 1473 EDITION OF 1 NOV 65 IS OBSOLETE
S/N 0102-LF-014-6601

UNCLASSIFIED

SECURITY CLASSIFICATION OF THIS PAGE (When Data Entered)

188762

Abstract

In a computer simulation particles of various energies were followed along their orbits to determine the probability of their absorption during one encounter with an inner satellite of Saturn, giving special consideration to leapfrog and corkscrew escape factors. The time interval between encounters may then be used to yield a measure of particle lifetimes in given satellite L shells. Energy and pitch angle dependence of satellite sweeping efficiency is illustrated. As expected, the small gyroradius electrons are completely absorbed in one satellite encounter, while the large gyroradius protons exhibit varying degrees of depletion.

Introduction

In Saturn's inner magnetosphere a combination of trapped particle longitudinal drift motion and satellite orbital motion will cause those particles found in a satellite's L shell to regularly encounter that satellite, which absorbs some fraction of the particles with each encounter. A particle's probability of absorption during one satellite encounter can be combined with the time between successive encounters to estimate particle lifetime in that satellite L shell, a helpful parameter for any radial diffusion considerations. Previous calculations along these lines were done by Thomsen [1977; 1979] and Mead & Hess [1973] among others for the satellites of Jupiter -- in cases of a "snowplow" effect where the satellite completely clears its L shell with one sweep, and a "random" effect where non-equatorially mirroring particles have a bounce period long enough or relative drift fast enough that they may escape absorption by drifting past the satellite during an extremity of their magnetic latitude excursion, also known as "leapfrogging" (see figure 3).

Although not considered at Jupiter, the smaller diameters of Saturn's satellites and the weaker magnetic field cause an additional escape mechanism to become appreciable, viz. the "corkscrew" effect, whereby the gyroradius and pitch angle of a particle allow its gyrocenter to pass within the effective satellite radius without the particle necessarily being absorbed. Absorption is assumed to take place only if the particle itself passes within the geometric satellite

radius, which will depend on the phase of the particle's helical path (figure 1).

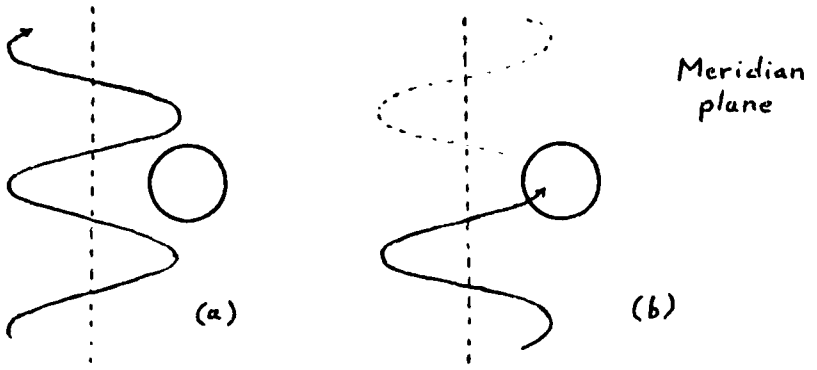

Figure 1: (a) Corkscrew escape, particle not absorbed.
(b) Different phase, particle absorbed.

Sample comparison of factors: 2 MeV protons at Mimas.

Satellite radius	180 km	
Proton gyroradius	262 km	for $\alpha_{eq} = 60°$
Effective radius	442 km	
Bounce period, T_B	30.6 sec	for $\alpha_{eq} = 60°$
Drift in $T_B/2$	944 km	

1. Snowplow profile --

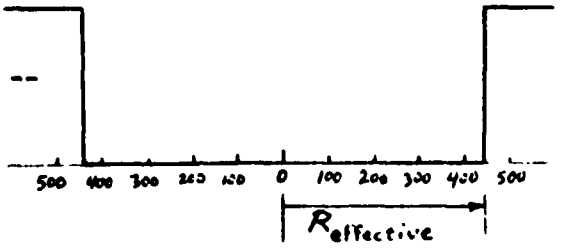

All particles with gyrocenters inside of $R_{effective}$ are removed.

2. Leapfrog profile -- Thomsen [1977] reduces the absorption by a factor of $\alpha_D = \frac{2 \times R \text{ effective}}{\text{drift in } T_B/2}$, or more precisely, $\alpha_D(x) = \frac{\text{chord length at } x}{\text{drift in } T_B/2}$.

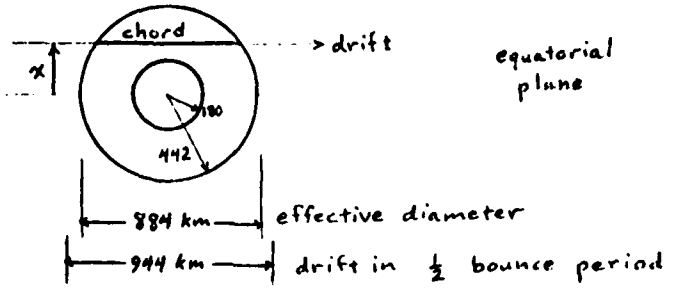

The result for 2 MeV protons ($\alpha_{eq} = 60°$) at Mimas is --

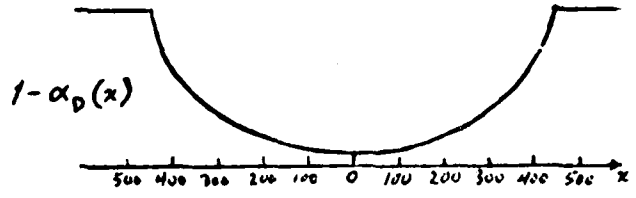

3. Addition of corkscrew effect -- refer to figure 1, drawn for 2 MeV protons ($\alpha_{eq} = 60°$) at Mimas. A computer tally of the absorption of differently phased particles yields the following profile for the combined effect of both leapfrog and corkscrew factors --

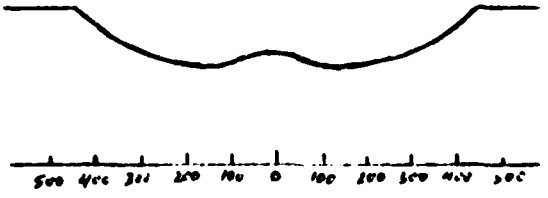

The other escape mechanism which was considered at Jupiter arises from the inclination of a satellite's orbit with respect to the magnetic equator, allowing near-equatorially mirroring particles to slip by during much of the satellite's orbit. This effect is minimal at Saturn, as its inner satellites always remain very near the magnetic equator and will continuously be able to intercept even the near-equatorially mirroring particles.

A zero offset, zero tilt dipole magnetic field model is adopted for the computations in this report and the inner satellites are then assumed to remain on the magnetic equator (zero inclination orbits), slight approximations which do not significantly affect the outcome.

The effect of satellite orbit eccentricity on particle lifetimes is discussed in a later section.

The profiles presented in this report show the probability for a particle to escape absorption on one passing of the satellite, plotted against the difference in radial distance between the center of the satellite and the gyrocenter of the particle (expressed in kilometers). While they qualitatively resemble absorption "signatures" it should be stressed that these profiles indicate gyrocenter depletions. In the dynamical situation those particles seen in a satellite signature by an omnidirectional detector may be displaced radially anywhere up to one gyroradius from their gyrocenters, a smearing effect, and in practice the satellite has of course interacted with the particles many times, so care must be taken in relating these profiles to the observed particle flux measurements.

Calculational Details and Discussion

The expressions, parameters and constants used in this analysis are taken directly from Thomsen and Van Allen [1980]. In particular:

Dipole moment of Saturn = M = 0.20 gauss R_s^3 , zero offset, zero tilt.

Keplerian orbital angular velocity of satellite

$$\omega_k = \frac{4.1905 \times 10^{-4}}{a^{3/2}} \left(1 + \frac{0.0125}{a^2}\right) \text{ , } a \text{ in units of } R.$$

Planetary rotational angular velocity = $\Omega = 1.637 \times 10^{-4}$ rad/sec corresponding to a rotational period of 10 hrs 39.9 min.

Averaged longitudinal particle drift rate (rotating reference frame)

$$\omega_D = \pm\, 2.083 \times 10^{-5}\, L\, E \left(\frac{E + 2mc^2}{E + mc^2}\right)\left(\frac{F}{G}\right)$$

+ for protons (eastward), − for electrons (westward)

where $$\frac{F}{G} = \frac{1}{1.04675 + 0.45333 \sin^2\lambda_m - 0.04675 \exp(-6.34568 \sin^2\lambda_m)}$$

or from Schultz and Lanzerotti [1974],

$$\frac{F}{G} = \frac{5.5208 - 0.4381 \sin\alpha_{eq} - 0.6396 \left[\sin\alpha_{eq} \ln \sin\alpha_{eq} + \sqrt{\sin\alpha_{eq}}\right]}{6 * \left[1.3802 - 0.3198 \left(\sin\alpha_{eq} + \sqrt{\sin\alpha_{eq}}\right)\right]}.$$

Particle angular velocity relative to satellite = $\omega_{rel} = \Omega + \omega_D - \omega_k$

Time interval between successive encounters of the particle with the satellite = $T_E = 2\pi / |\omega_{rel}|$

Bounce period = $$T_B = 0.8006 \frac{L(E+mc^2)}{[E(E+2mc^2)]^{1/2}} \cdot H(\alpha_{eq})$$

where $H(\alpha_{eq}) = 1.38 - 0.32(\sin\alpha_{eq} + \sin^{1/2}\alpha_{eq})$

Satellite parameters	L	Diameter
1979 S2/S4	2.528	170 km
Mimas	3.092	360
Enceladus	3.968	600
Tethys	4.913	1040
Dione	6.292	1000
Rhea	8.787	1600

Table 1: L values from Thomsen and Van Allen [1980]. Diameters from Cruikshank [1978], except 1979 S2/S4 from Van Allen, et. al. [1980a].

Separating bounce motion from drift motion the probability of a particle's absorption in one bounce past a satellite is computed as a function of distance between gyrocenter and satellite center. For a given energy and pitch angle a family of particle orbits, each differing in phase, is considered. The fraction of these intercepting the satellite body is the probability of such a particle's absorption (figure 2). (100 phases evenly spread over 2π radians are used in my computation.)

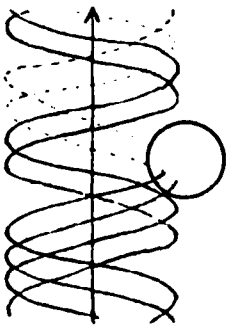

Figure 2: Particles of different gyrophase, some fraction absorbed. Fraction is a function of distance between gyrocenter and satellite center.

This probability is basically the corkscrew factor which, as suggested in the introduction, will modify the leapfrog profile.

A leapfrog profile may be computed in the same manner by considering a family of bounce motions past a satellite (figure 3), giving the same results as Thomsen's [1977] analytic expression cited earlier in this paper. (This would be the final result in the limit of zero gyroradius.)

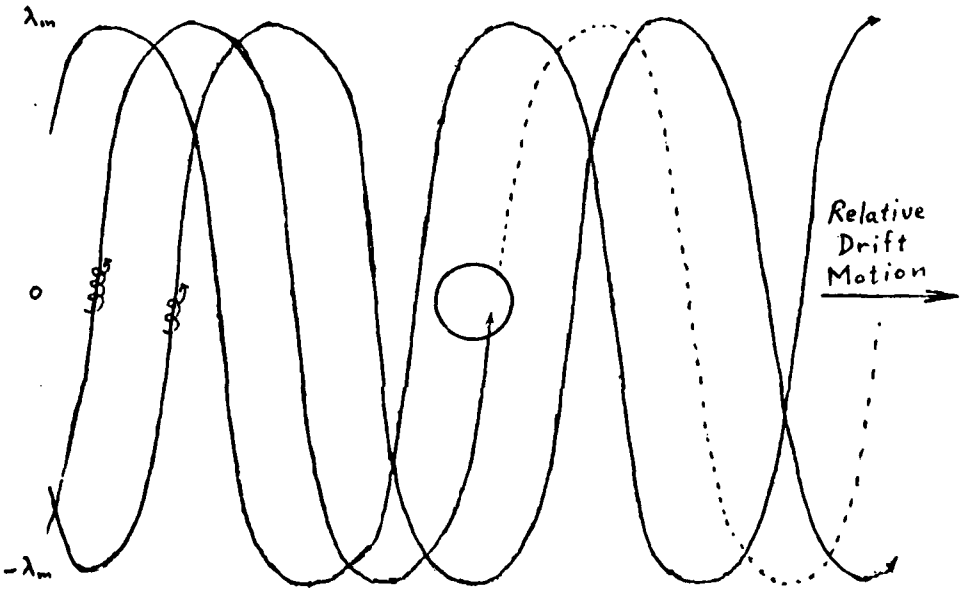

Figure 3: Plane of constant L. Gyrocenter bounce motions as particles drift. Gyrocenters intercepting satellite are removed in limit of zero gyroradius.

To introduce the corkscrew factor into the leapfrog picture the gyrocenter paths which pass within the satellite's effective radius are weighted by the appropriate corkscrew factor (function of distance from satellite center). Thus the curves shown in figure 3, there considered either to be absorbed or to get past, are now assigned

probabilities of getting past the satellite, say 0.9, 0.4, 0.1, and 0.6 for example (figure 4).

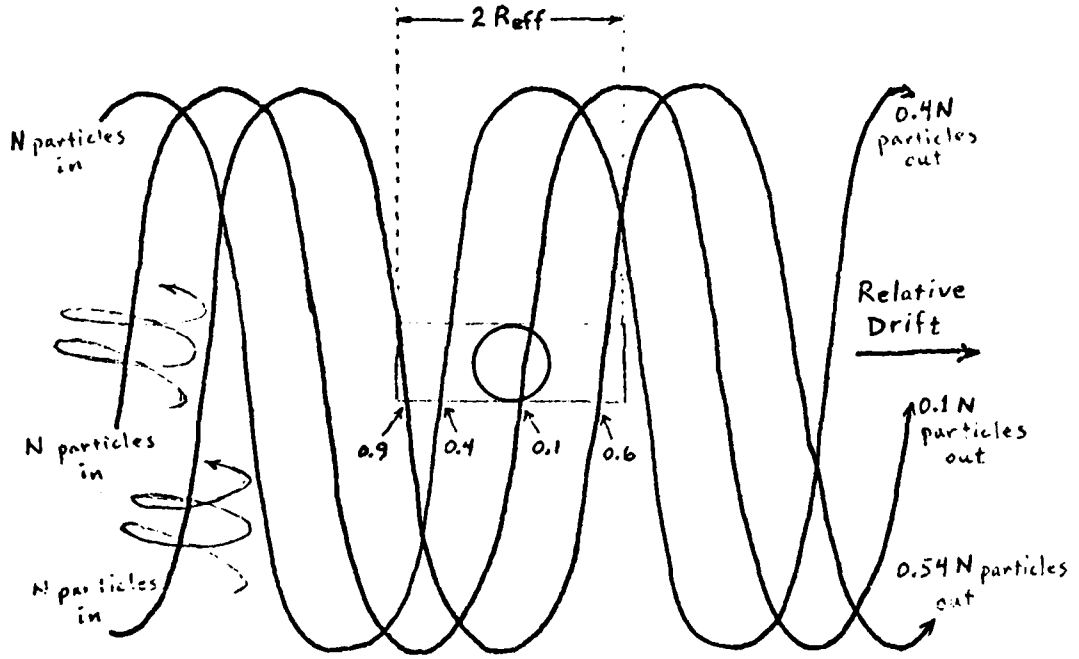

Figure 4: Plane of constant L. Gyrocenter bounce motions as particles drift. Gyrocenter paths assigned escape probabilities in non-zero gyroradius case.

The product of the probabilities is taken for a curve passing within the effective radius more than once, e. g. figure 4 where 0.9 x 0.6 gives 0.54 for one curve. The average of these probabilities for many (again I use 100 phases) such curves spread evenly in phase will give the fraction of particles from an initial population which survive one satellite encounter -- accounting for both leapfrog AND corkscrew escape mechanisms together.

When calculated for several values of ΔL ranging over $\pm R_{effective}$ from the nominal satellite L shell (figure 5), the results may be plotted as a gyrocenter absorption profile (figure 6), fraction of particles remaining vs. ΔL.

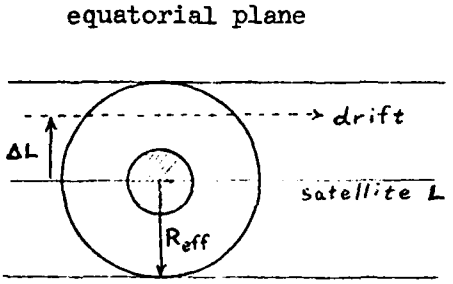

Figure 5: Gyrocenter drift path across absorption region.

Table 2:
Energy values examined (MeV)

Electrons	Protons	
0.1	0.1	5.0
1.0	0.2	10.0
10.0	0.5	20.0
20.0	1.0	40.0
30.0	2.0	80.0

This was done for electrons and protons of various energies (Table 2) at the six satellite positions given in table 1. The plots each contain results for 9 different pitch angles (equatorial) and are explained in the example of figure 6.

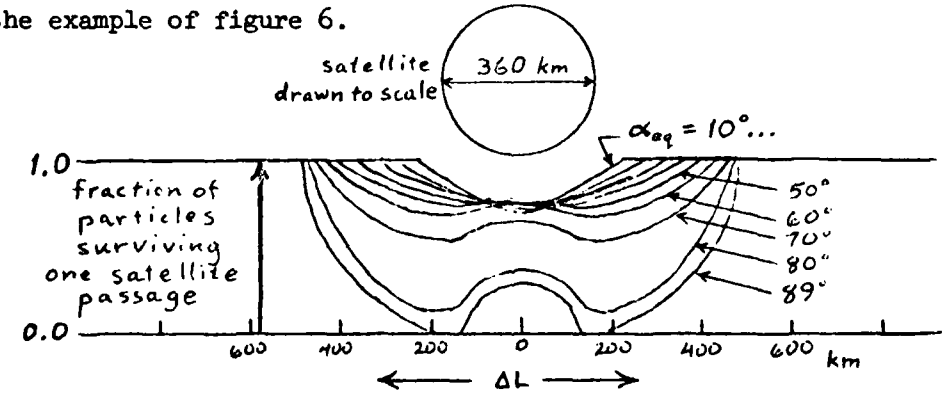

Figure 6: 2.0 MeV protons at Mimas, L = 3.092, sat. radius = 180 km, pitch angles α_{eq} = 10, 20, 30, 40, 50, 60, 70, 80, 89°.

Such a plot clearly shows the progression of larger gyroradii (hence effective satellite radius) with larger α_{eq}. (The omission of $\alpha_{eq} = 90°$ avoids undue complications in the computer program. The resulting profile would be indistinguishible from that of the $\alpha_{eq} = 89°$ substitution.)

Also apparent is a sudden trend toward deeper absorption at pitch angles greater than 70°. Intuitively one can reason that this sets in as the vertical distance between corkscrew "threads" becomes comparable with the satellite geometric diameter and the corkscrew escape effect is lost. For the Mimas example this is verified in table 3, where the distance in question is listed under h. Note also that the bounce time is reduced at larger pitch angles, but the relative velocity is correspondingly increased, so there is no appreciable net effect on the leapfrog escape mechanism (see table 3).

α_{eq}	h	T_B	ω_{rel}	$\omega_{rel} T_B L R_s/2$
10°	1871 km	45.2 s	.000280/s	1174 km
20	1785	41.1	.000294	1120
30	1645	37.7	.000305	1068
40	1455	34.8	.000316	1021
50	1221	32.5	.000325	979
60	950	30.6	.000333	944
70	650	29.2	.000339	918
80	330	28.4	.000343	902
89	33	28.1	.000344	896

Table 3: 2.0 MeV protons at Mimas, sat. diameter = 360 km. Vert. dist. between gyrations = h, affects corkscrew factor. Rel. drift in 1/2 bounce = $\omega_{rel} T_B L R_s/2$, leapfrog effect.

A somewhat puzzling feature is that hump growing in the middle at larger pitch angles. Somehow such particles have a higher chance of surviving by passing directly through the center of the satellite. A clue is that the feature begins to show at $\alpha_{eq} = 40°$ and becomes more obvious as α_{eq} increases. Looking at gyroradius vs. pitch angle (Table 4), $\alpha_{eq} = 40°$ is where the gyroradius first exceeds the satellite geometric radius of 180 km.

α_{eq}	gyroradius
10°	53 km
20	103
30	151
40	194
50	232
60	262
70	284
80	298
89	302

Table 4:
Gyroradius vs. α_{eq}
2.0 MeV protons
at Mimas.

For α_{eq} greater than or equal to 40° the gyrocenter may pass directly through the center of the satellite without losing the particles to absorption. This is a type of corkscrew escape effect independent of the vertical thread spacing, and thus is not lost but actually enhanced at greater pitch angles.

So the qualitative features of these profiles are readily explicable. A survey of the full set shows:

1. Low energy electrons are subject to snowplow absorption.
2. High energy electrons exhibit the same features as intermediate energy protons explained above.
3. Low energy protons give leapfrog type profiles, little evidence of corkscrew escape.
4. High energy protons are virtually unaffected by one satellite passage.

These observations are compatible with the given particle's gyroradius and relative drift velocity.

Low energy electrons, for example, have gyroradii much less than the satellite radius and have a very small relative drift, thus their gyrations and bounces are both too small to avoid absorption, and the satellite leaves a snowplow type profile.

High energy protons with their leaps and corkscrews on the order of thousands of kilometers will hardly notice a 360 km satellite. 80 MeV protons at Mimas have gyroradii up to 1950 km, drift 4500 to 5000 km per half bounce, and have several thousand kilometer spacing of their helix threads (pitch angle dependent of course). Only one or two percent of these particles are absorbed in one satellite passage. Therefore it would take many satellite passages to give the high energy proton depletion seen by Pioneer 11 instrumentation in the vicinity of Mimas' orbit. Moreover, the radial diffusion coefficient of these particles

must be small enough that the signature is not appreciably filled in over the time interval between satellite passages. This time interval, given previously as $T_E = 2\pi/|\omega_{rel}|$, is about 12 minutes for 80 MeV protons at Mimas. With an exactly circular orbit it would take Mimas N passages to sweep up half of the 80 MeV protons, where $0.98^N = 1/2$; $N = 34.3$, giving a measure of particle lifetime 34.3 x 12 minutes = ~412 minutes.

However, the slight eccentricity of the satellites' orbits cause them to sweep larger regions than merely $\pm R_{effective}$ from their nominal L shell. As this sweeping region is broadened the lifetimes of particles will increase proportionately. E. g. between apo- and periapsis Mimas will undergo a radial excursion of ~8000 km and so will sweep a region 8000 km + (2 x R_{eff}) wide. This is ~11500 km for 80 MeV protons (depending on α_{eq}), or ~ 3 times the area Mimas would sweep in a zero eccentricity orbit. Therefore particles should survive roughly 3 times longer on the average. For smaller gyroradius particles this factor increases, reaching ~ 22 (8000km/360km) as the gyroradius vanishes (low energy electrons).

Thomsen and Van Allen [1980] noted that T_E approaches infinity for electrons ~ 1 MeV, the so-called resonant energy. It is speculated that electrons near this energy would be able to diffuse across the satellite orbit unaffected during the large T_E intervals. [Van Allen, et. al., 1980b] Inwardly diffusing electrons of other energies would be swept up. More work on this form of energy filtering is in progress.

GYROCENTER ABSORPTION PROFILES

Electrons -- at S2, Mimas, Enceladus, Tethys, Dione, and Rhea
Protons -- at S2, Mimas, Enceladus, Tethys, Dione, and Rhea
Satellite diameter is indicated to scale at top of each page.

Detailed computer printout of these profile values is available on request to the author, listing additional parameters for each case, each α_{eq}.

-- gyroradius, effective radius, resolution of profile, relative drift frequency, drift in 1/2 bounce, vertical displacement in one gyration, gyrofrequency, and drift period T_E.

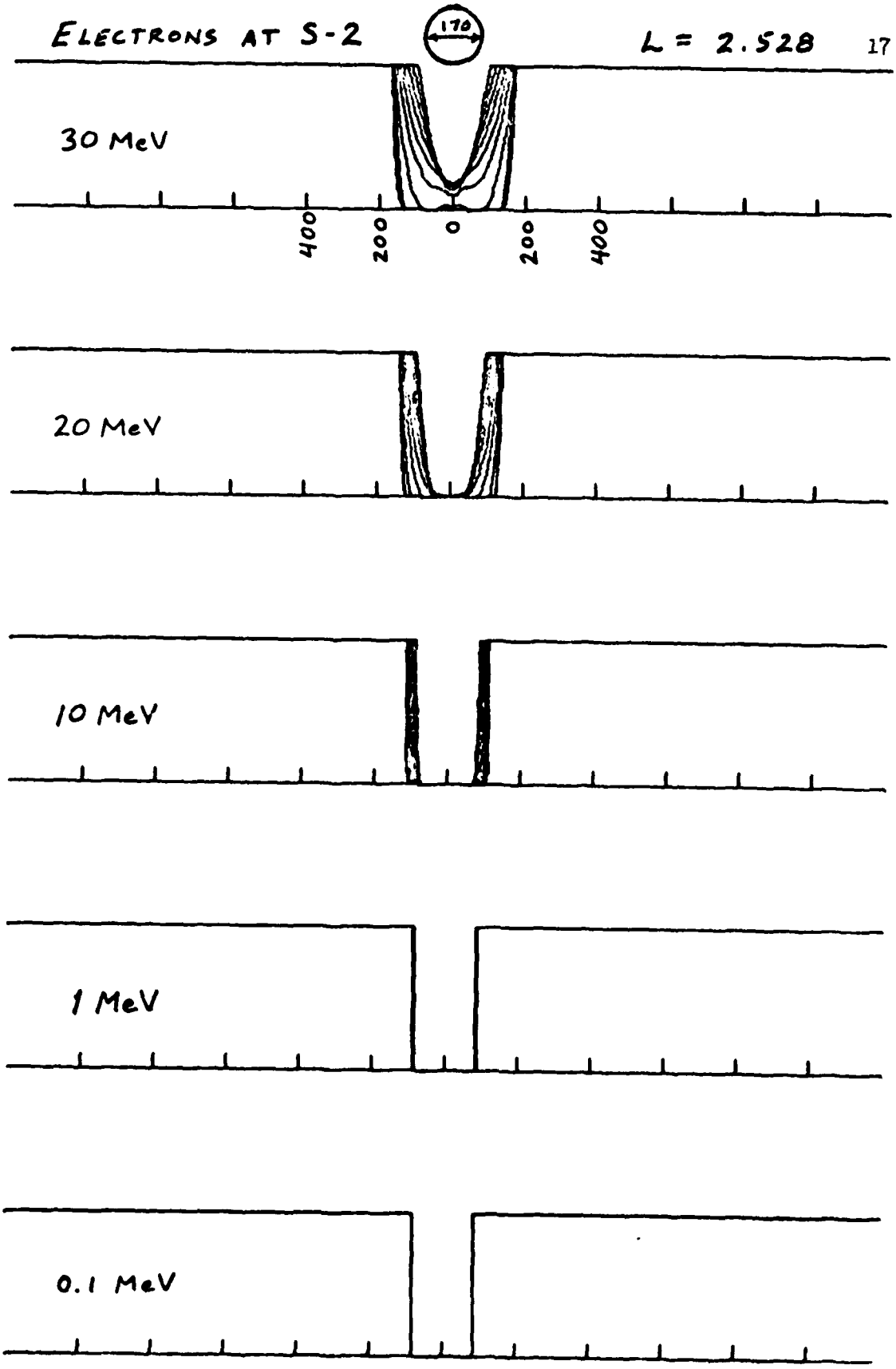
ELECTRONS AT S-2
170
L = 2.528
30 MeV
400
200
0
200
400
20 MeV
10 MeV
1 MeV
0.1 MeV

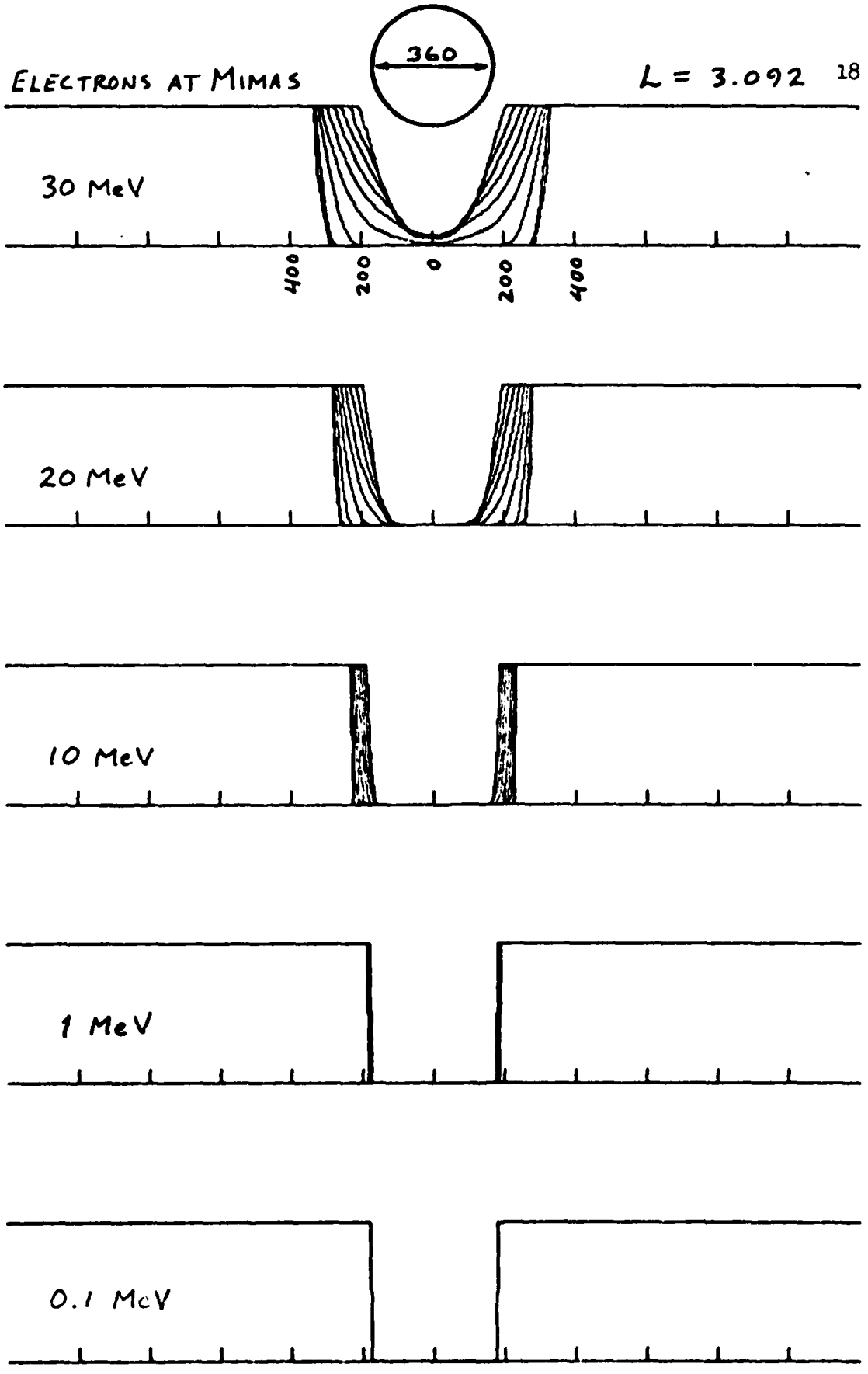
ELECTRONS AT MIMAS
360
L = 3.092
30 MeV
400
200
0
200
400
20 MeV
10 MeV
1 MeV
0.1 MeV

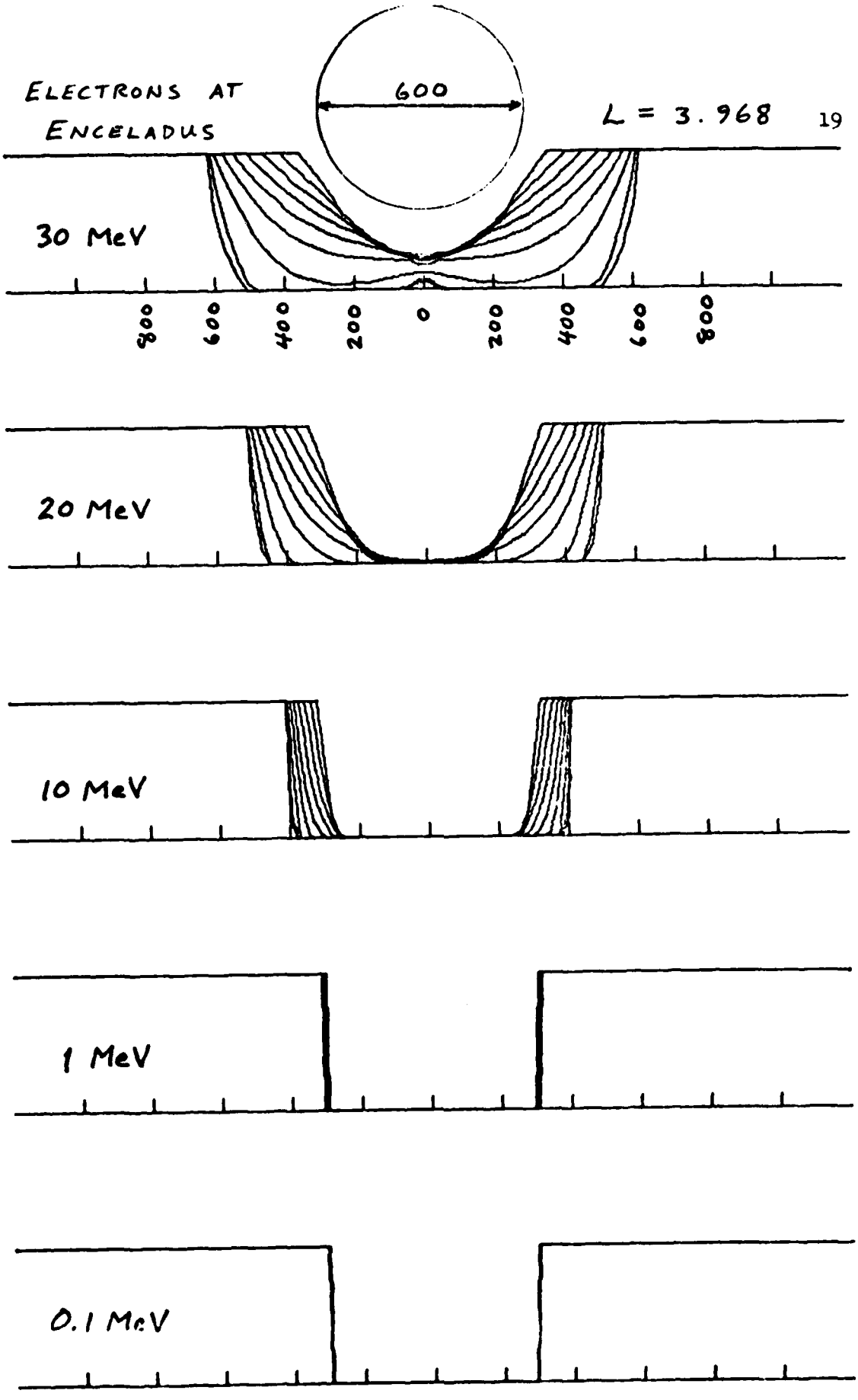
ELECTRONS AT ENCELADUS
600
L = 3.968
30 MeV
800
600
400
200
0
200
400
600
800
20 MeV
10 MeV
1 MeV
0.1 MeV

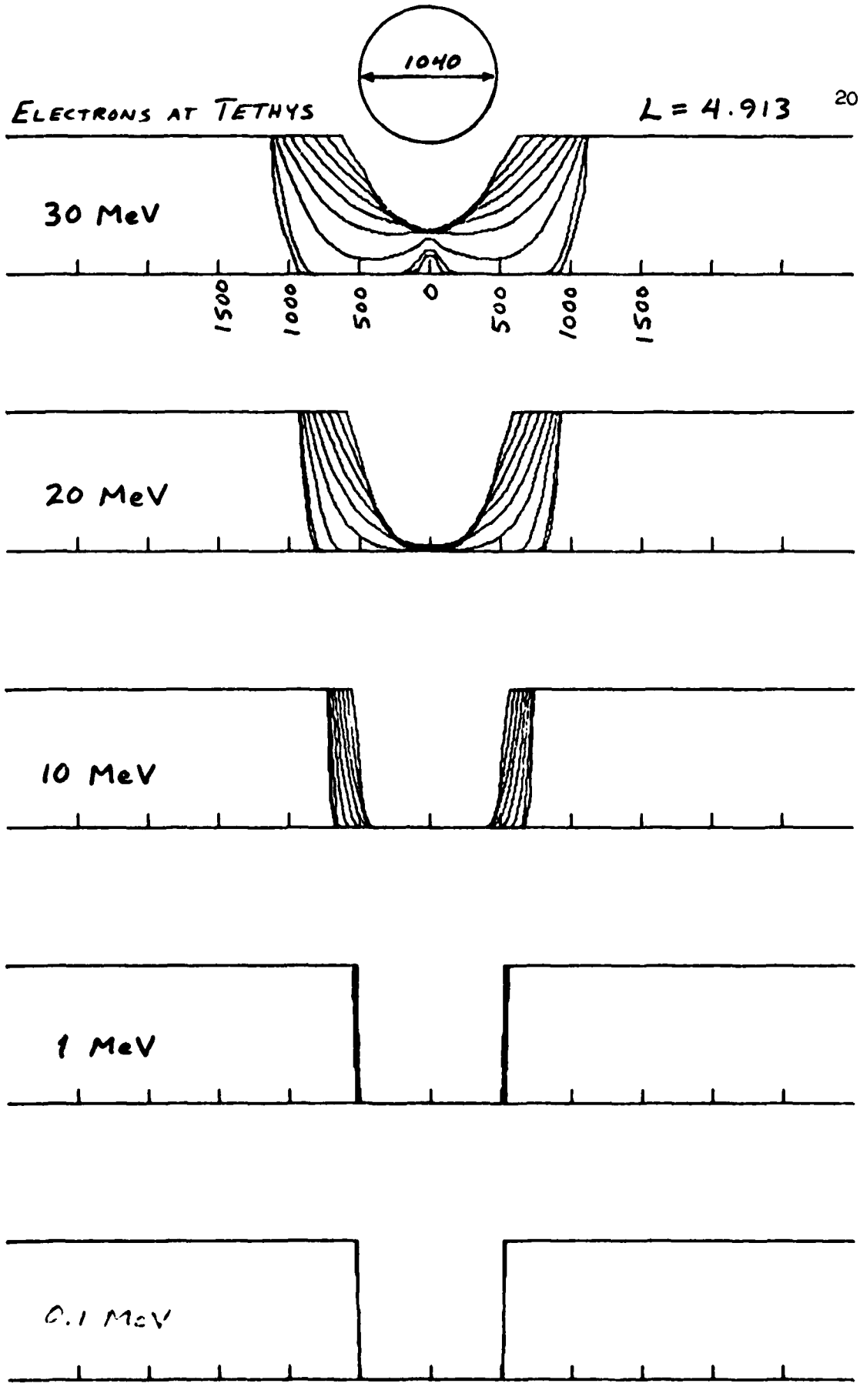
1040
ELECTRONS AT TETHYS
L = 4.913
30 MeV
1500
1000
500
0
500
1000
1500
20 MeV
10 MeV
1 MeV
0.1 MeV

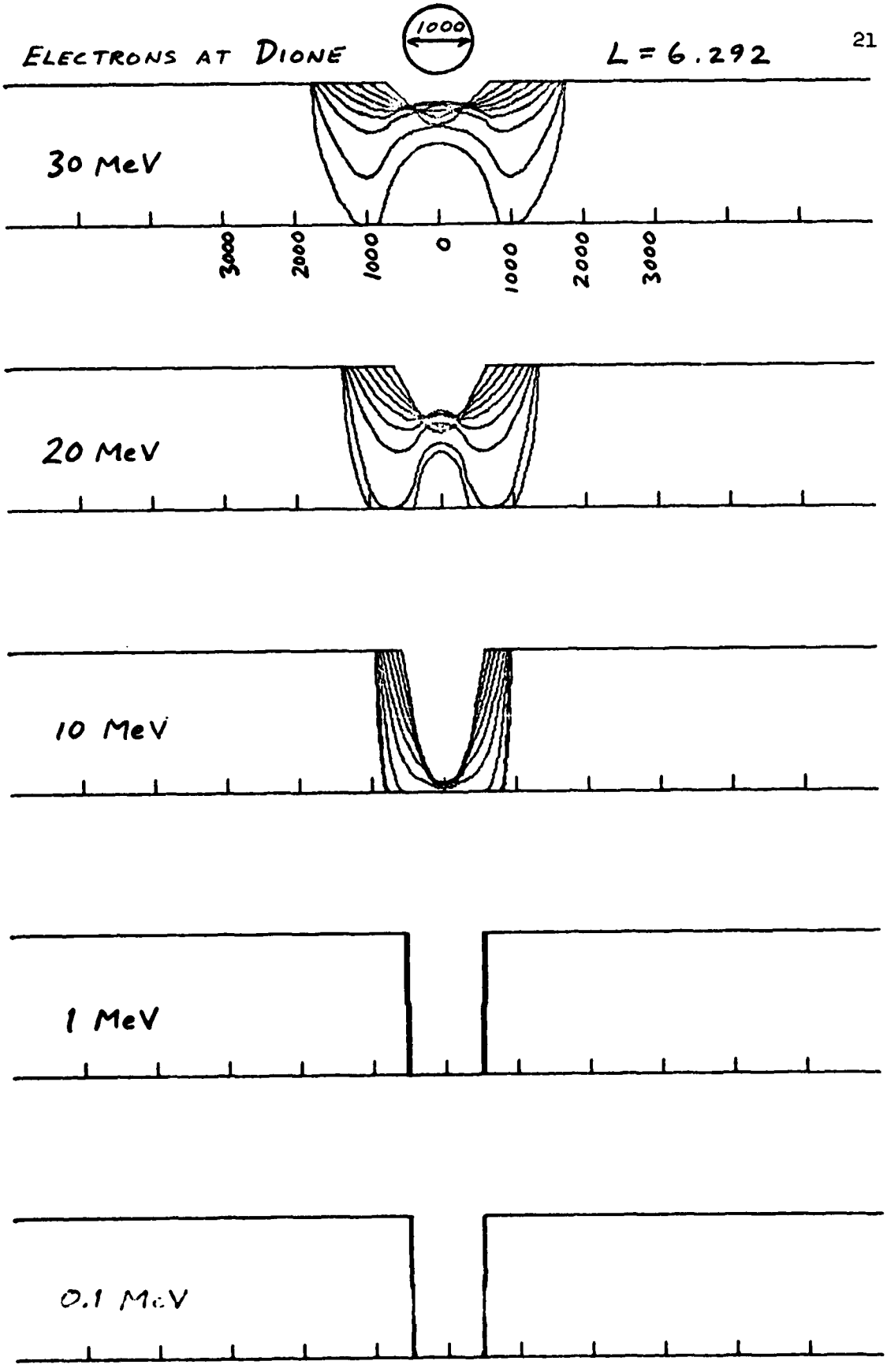
ELECTRONS AT DIONE
1000
L = 6.292
30 MeV
3000
2000
1000
0
1000
2000
3000
20 MeV
10 MeV
1 MeV
0.1 MeV

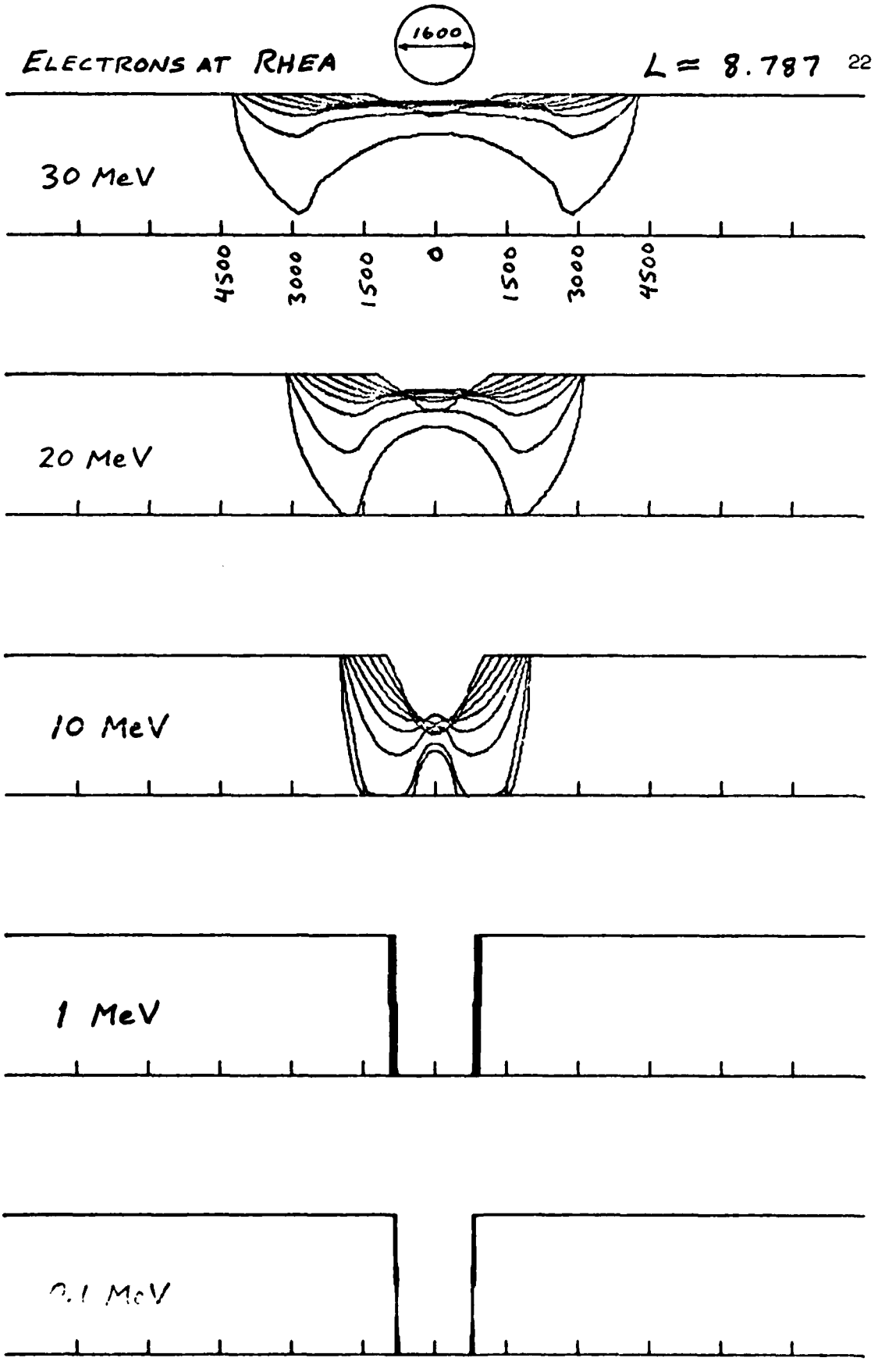
ELECTRONS AT RHEA
1600
L = 8.787
30 MeV
4500
3000
1500
0
1500
3000
4500
20 MeV
10 MeV
1 MeV
0.1 MeV

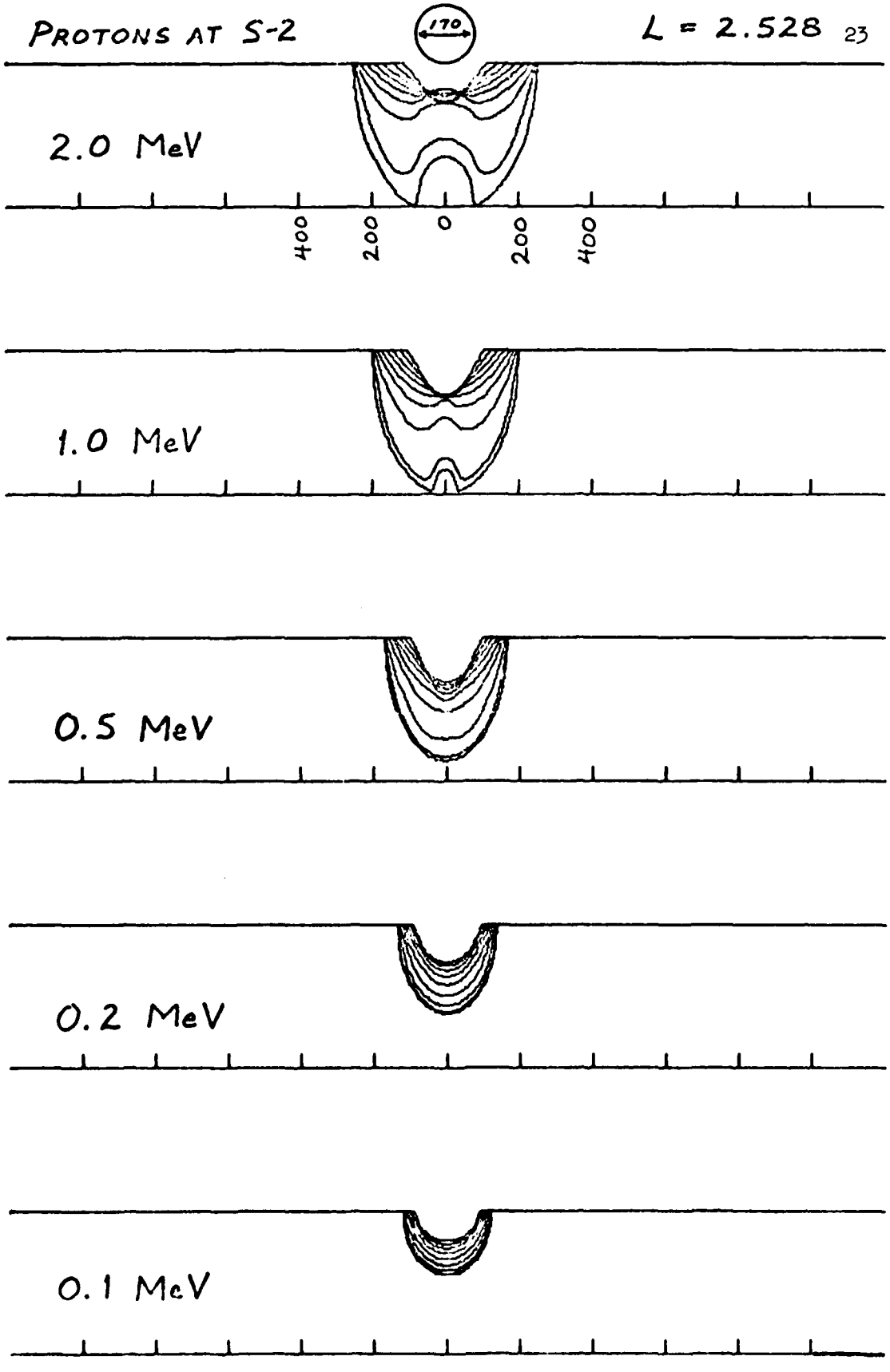
PROTONS AT S-2
170
L = 2.528
23
2.0 MeV
400
200
0
200
400
1.0 MeV
0.5 MeV
0.2 MeV
0.1 MeV

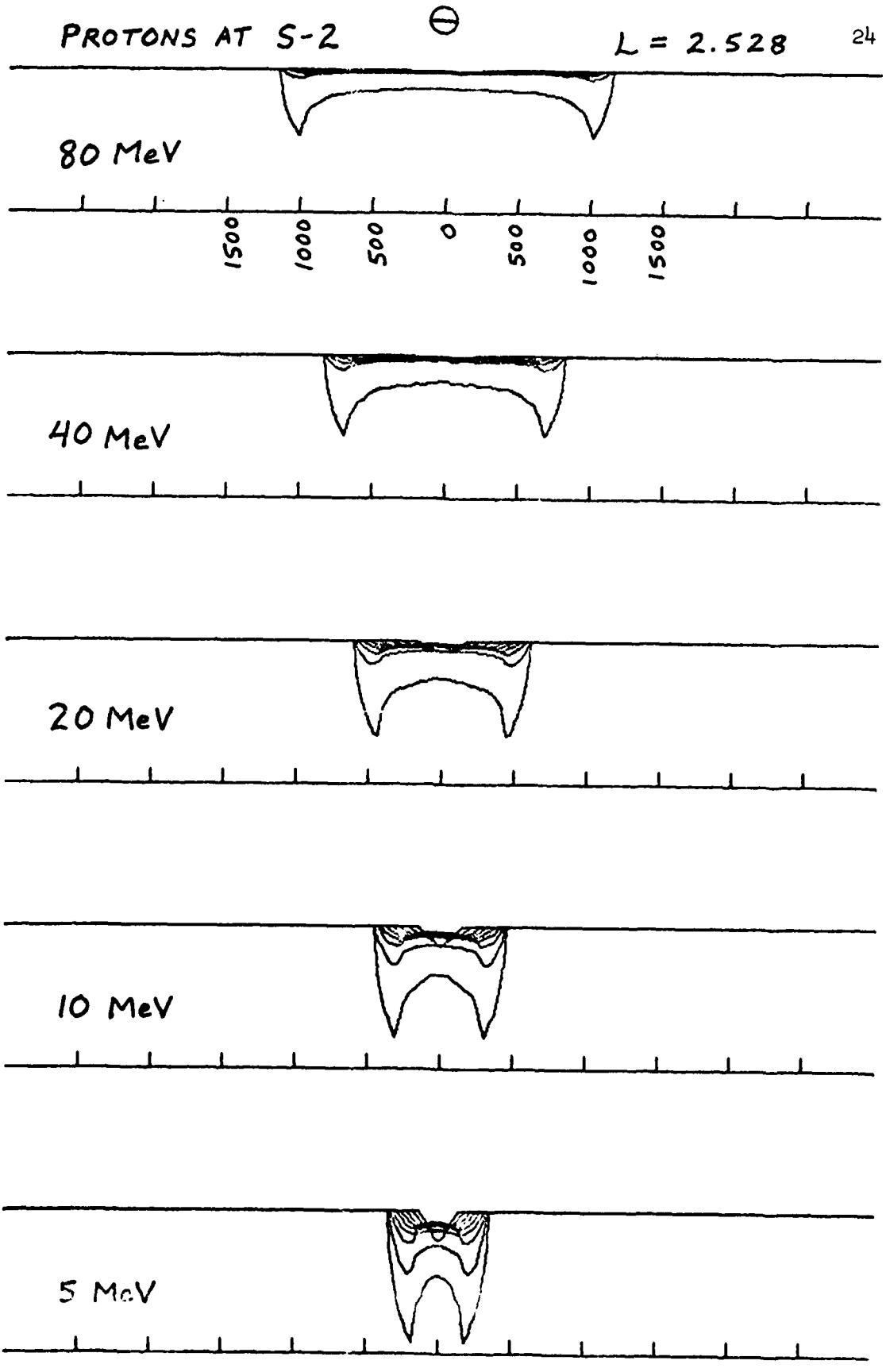
PROTONS AT S-2
Θ
L = 2.528
80 MeV
1500
1000
500
0
500
1000
1500
40 MeV
20 MeV
10 MeV
5 MeV

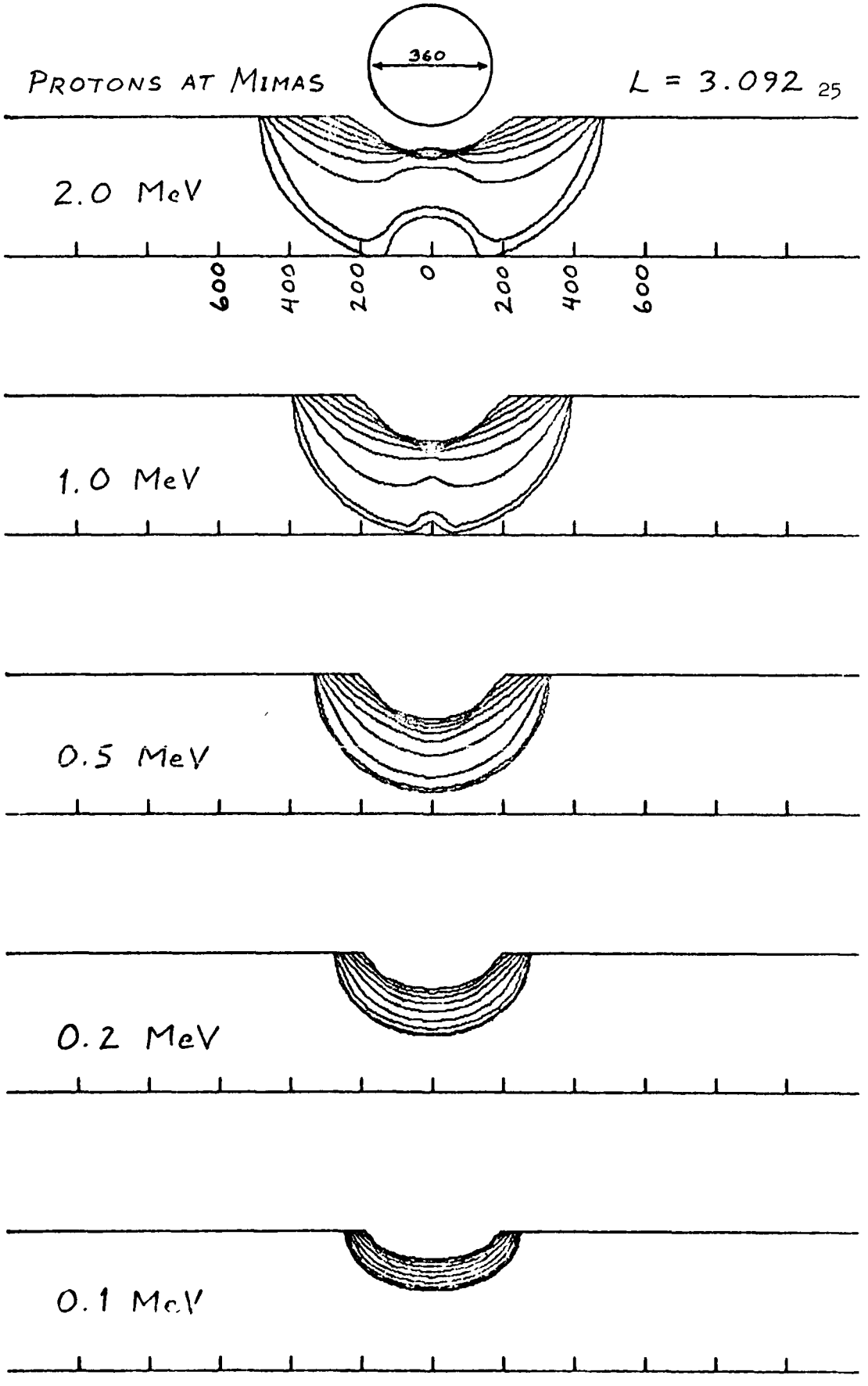
PROTONS AT MIMAS
360
L = 3.092
25
2.0 MeV
600
400
200
0
200
400
600
1.0 MeV
0.5 MeV
0.2 MeV
0.1 MeV

PROTONS AT MIMAS ⊖ $L = 3.092$

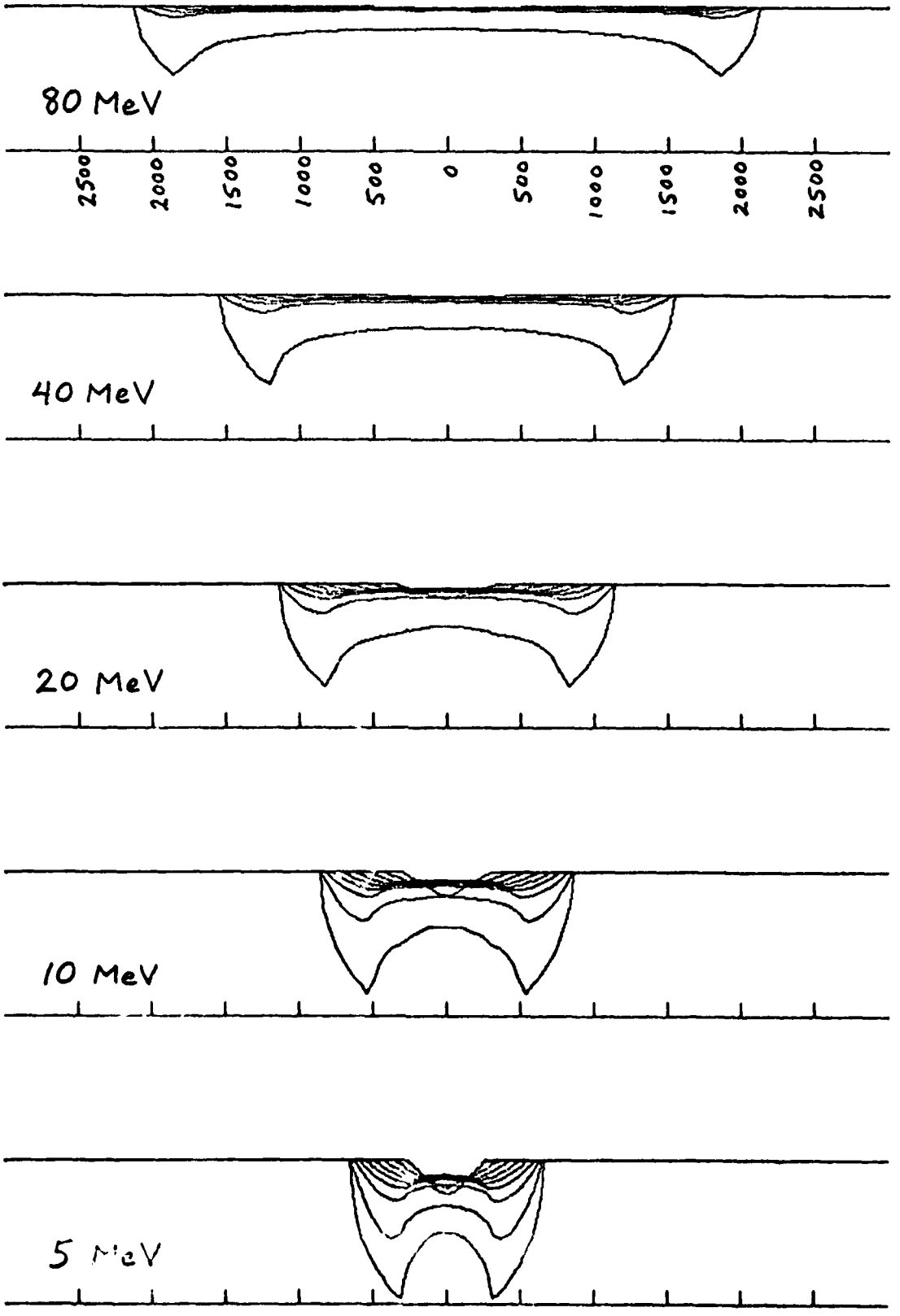

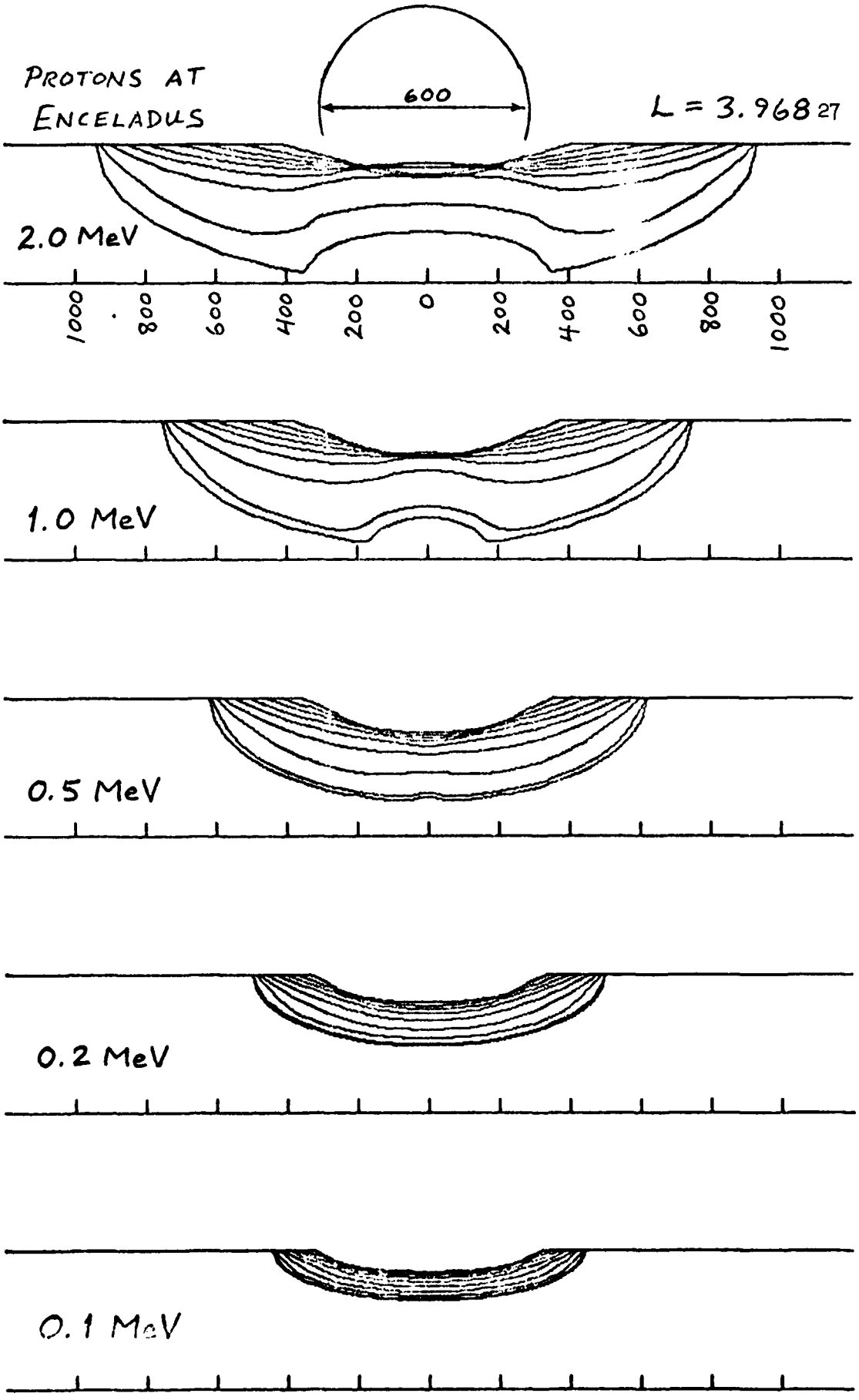
PROTONS AT
ENCELADUS
600
L = 3.968 27
2.0 MeV
1000
800
600
400
200
0
200
400
600
800
1000
1.0 MeV
0.5 MeV
0.2 MeV
0.1 MeV

PROTONS AT ENCELADUS ⊖ L = 3.968

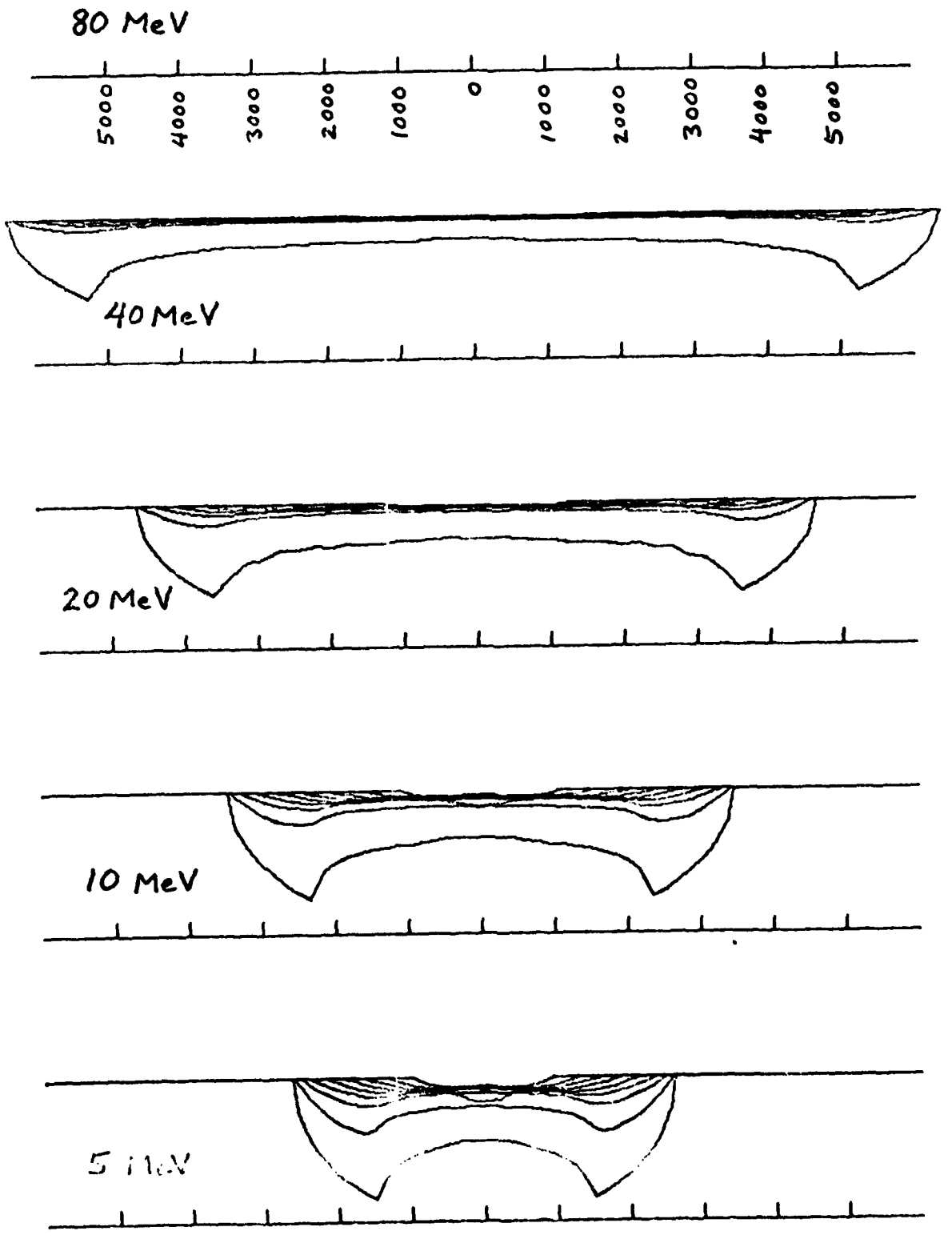

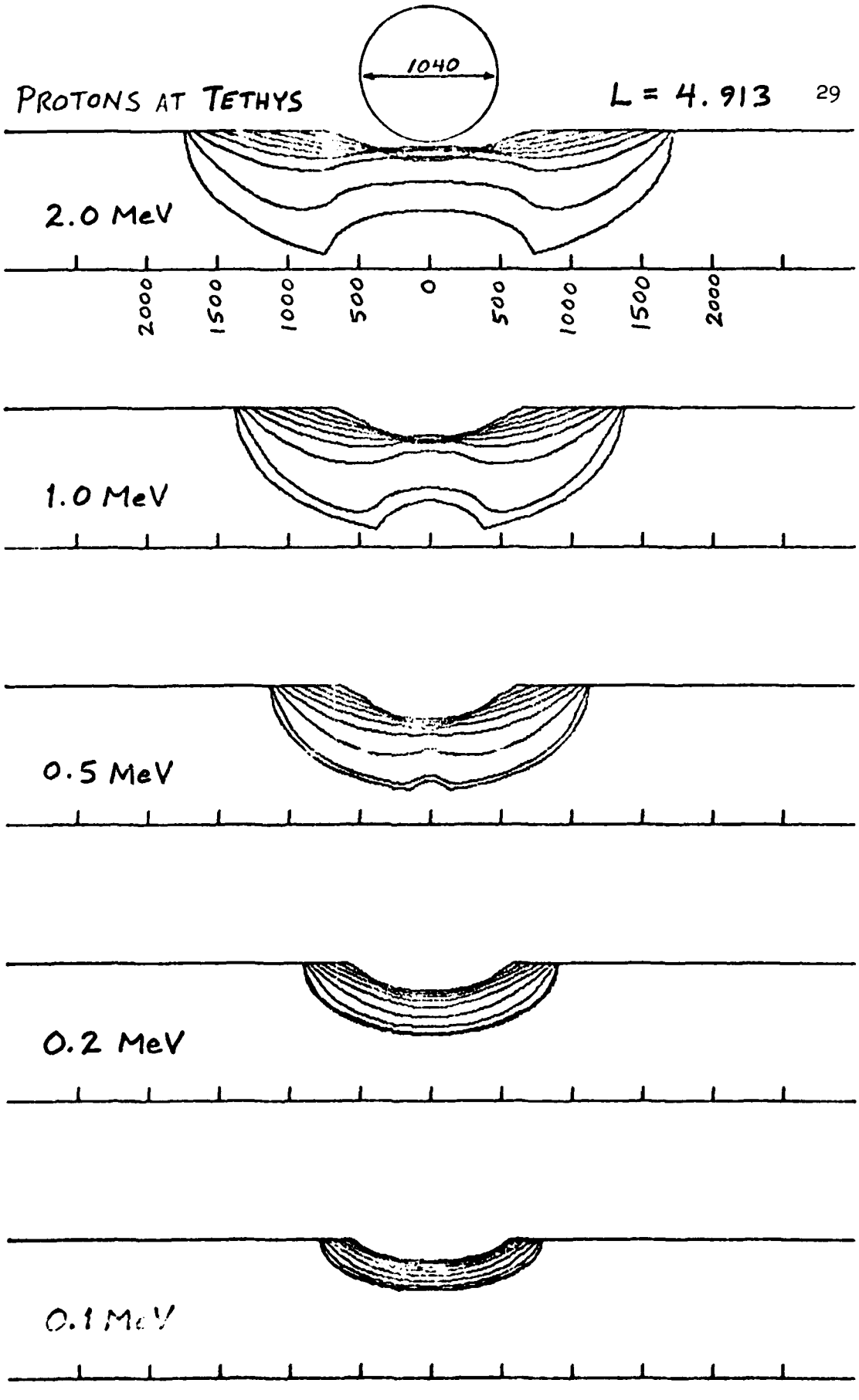
PROTONS AT TETHYS
L = 4.913
29
1040
2.0 MeV
2000
1500
1000
500
0
500
1000
1500
2000
1.0 MeV
0.5 MeV
0.2 MeV
0.1 MeV

PROTONS AT TETHYS ⊖ L = 4.913

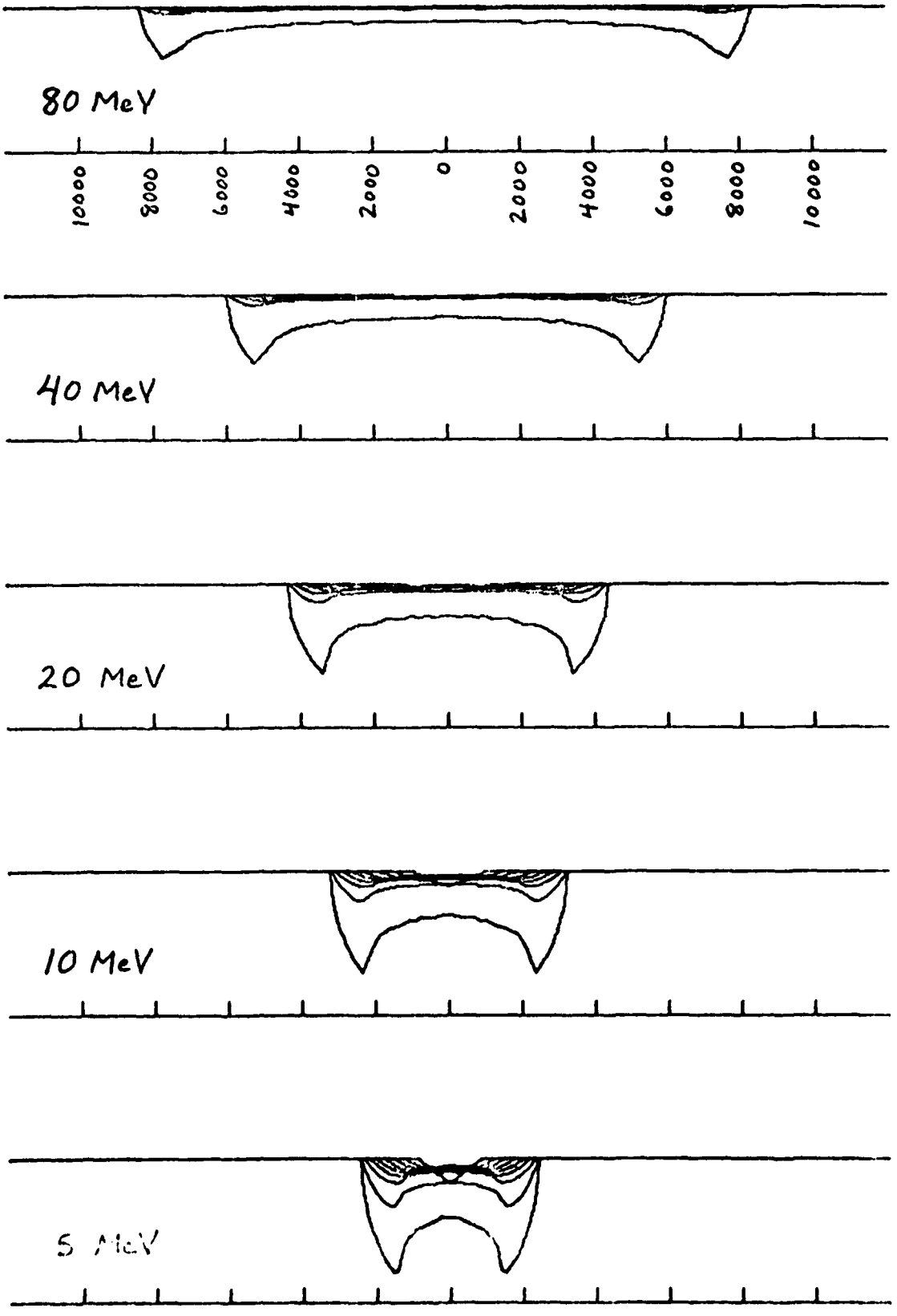

PROTONS AT DIONE

L = 6.292

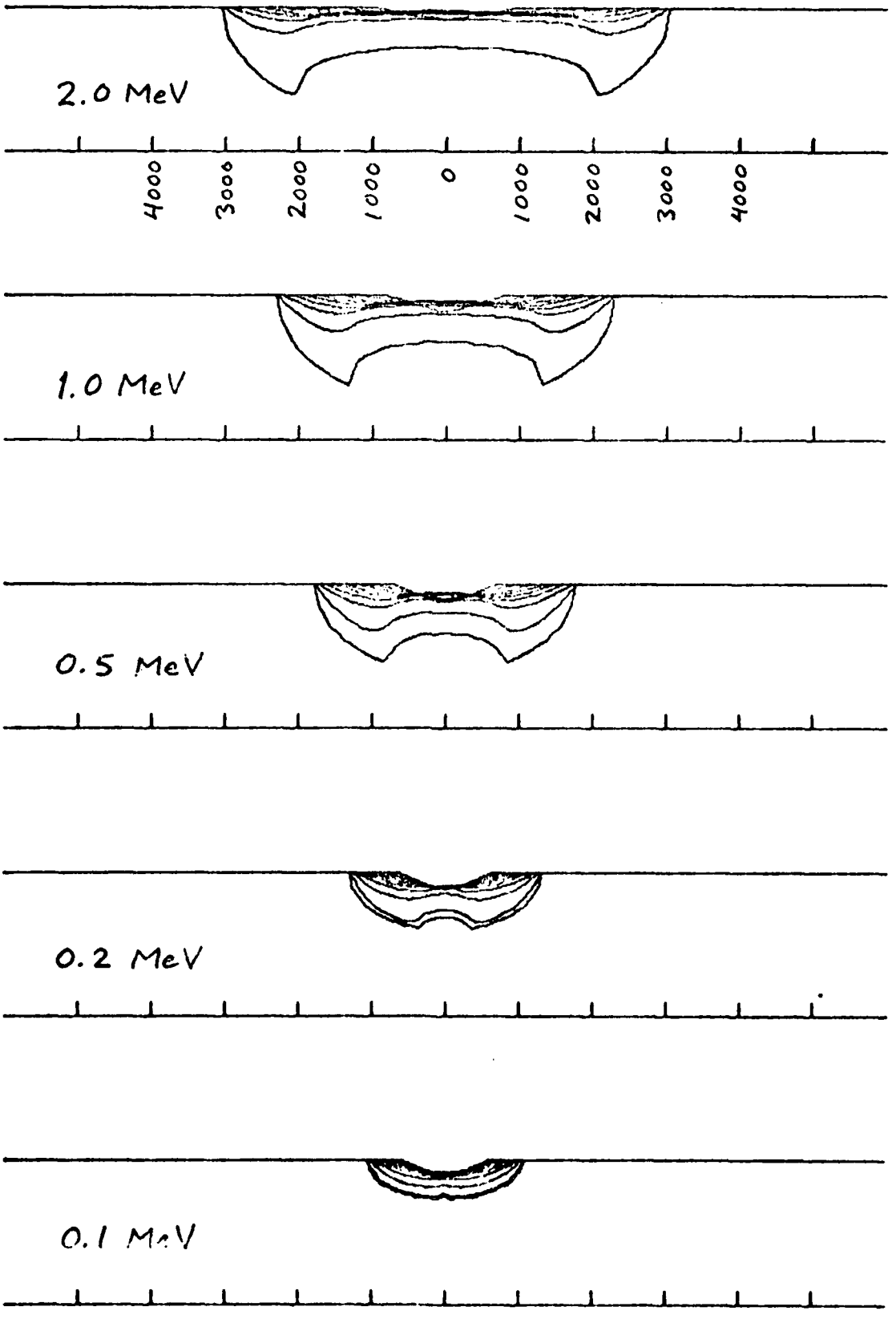

PROTONS AT DIONE Θ L = 6.292

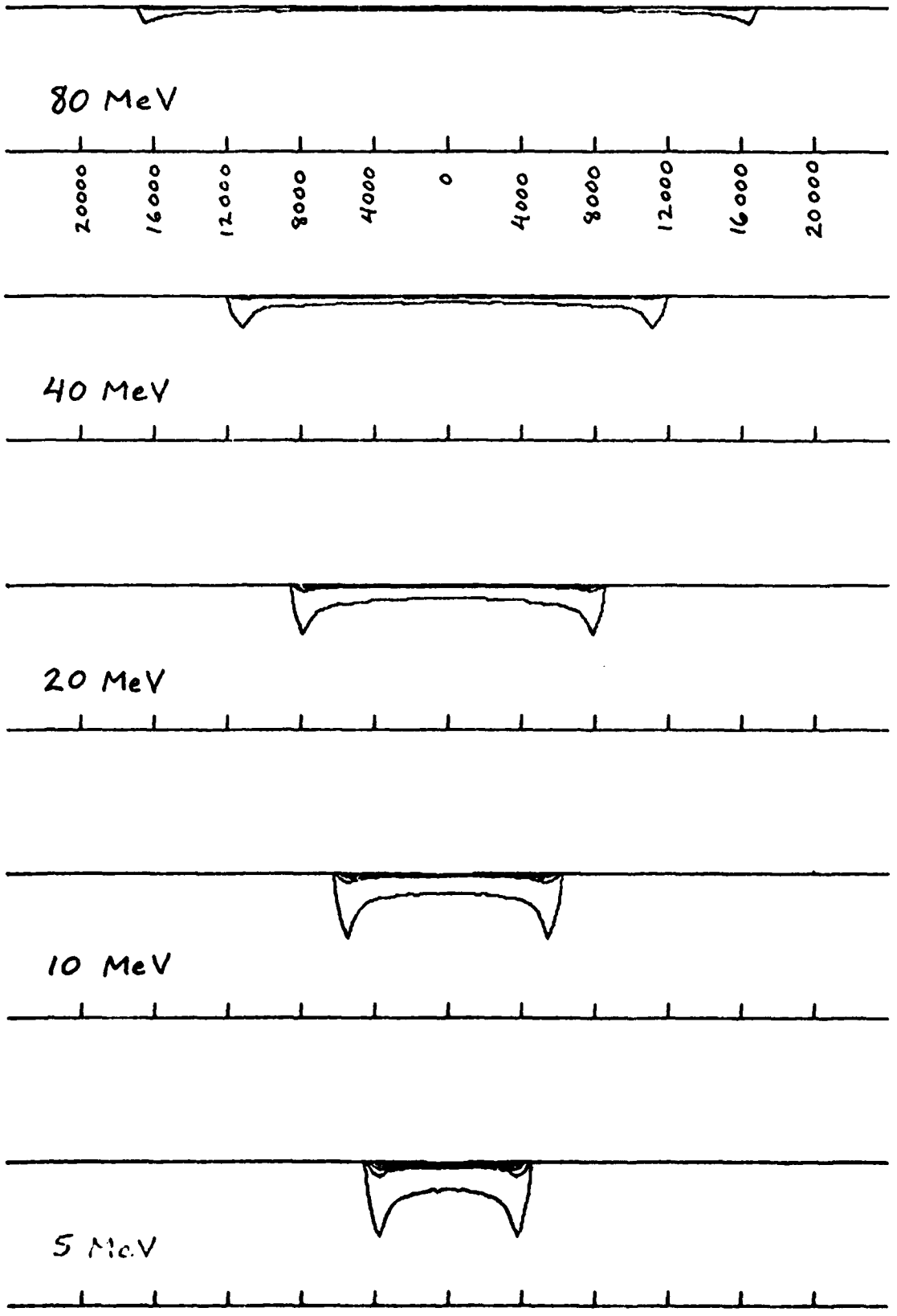

PROTONS AT RHEA

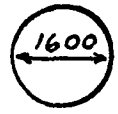

L = 8.787

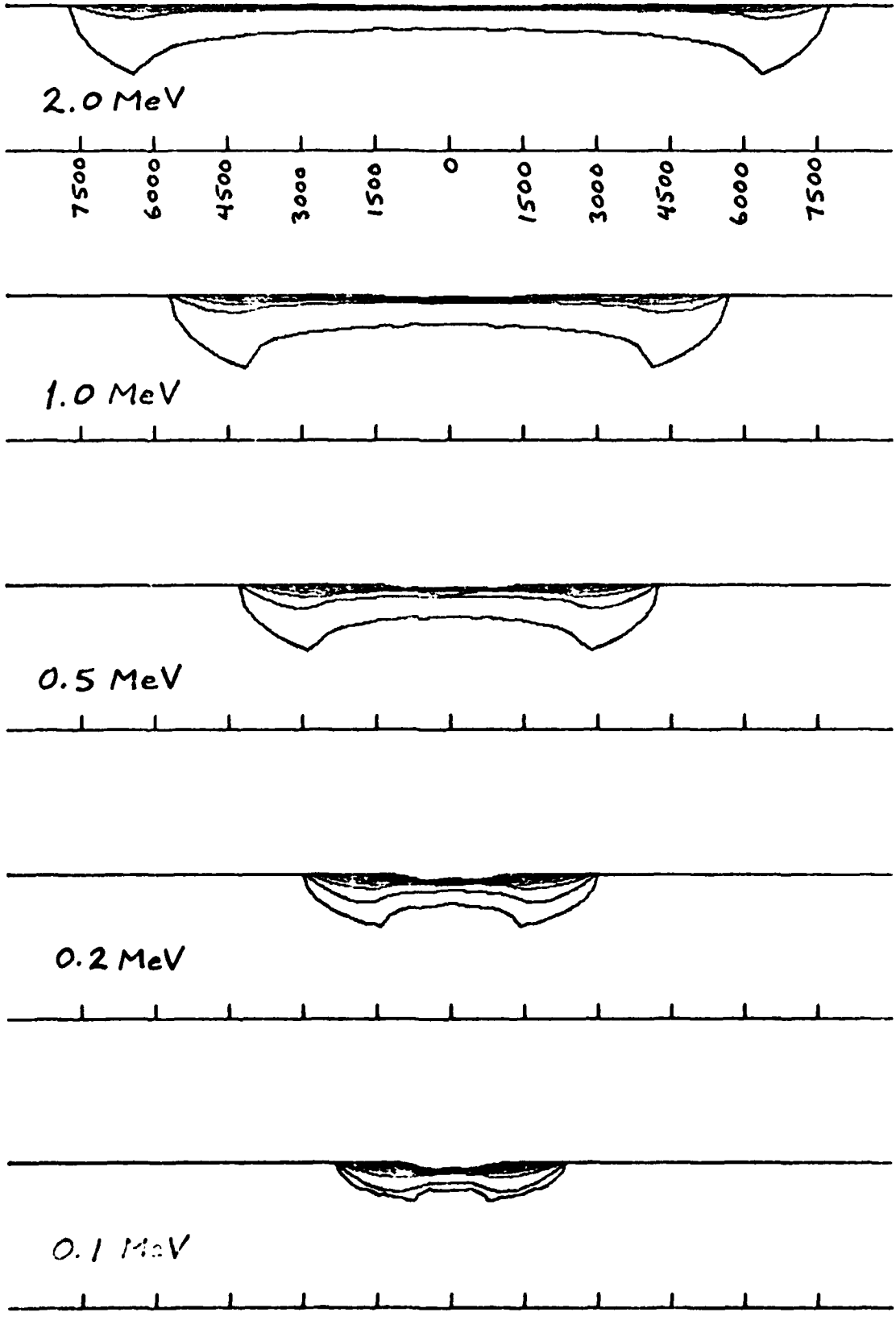

PROTONS AT RHEA Θ L = 8.787

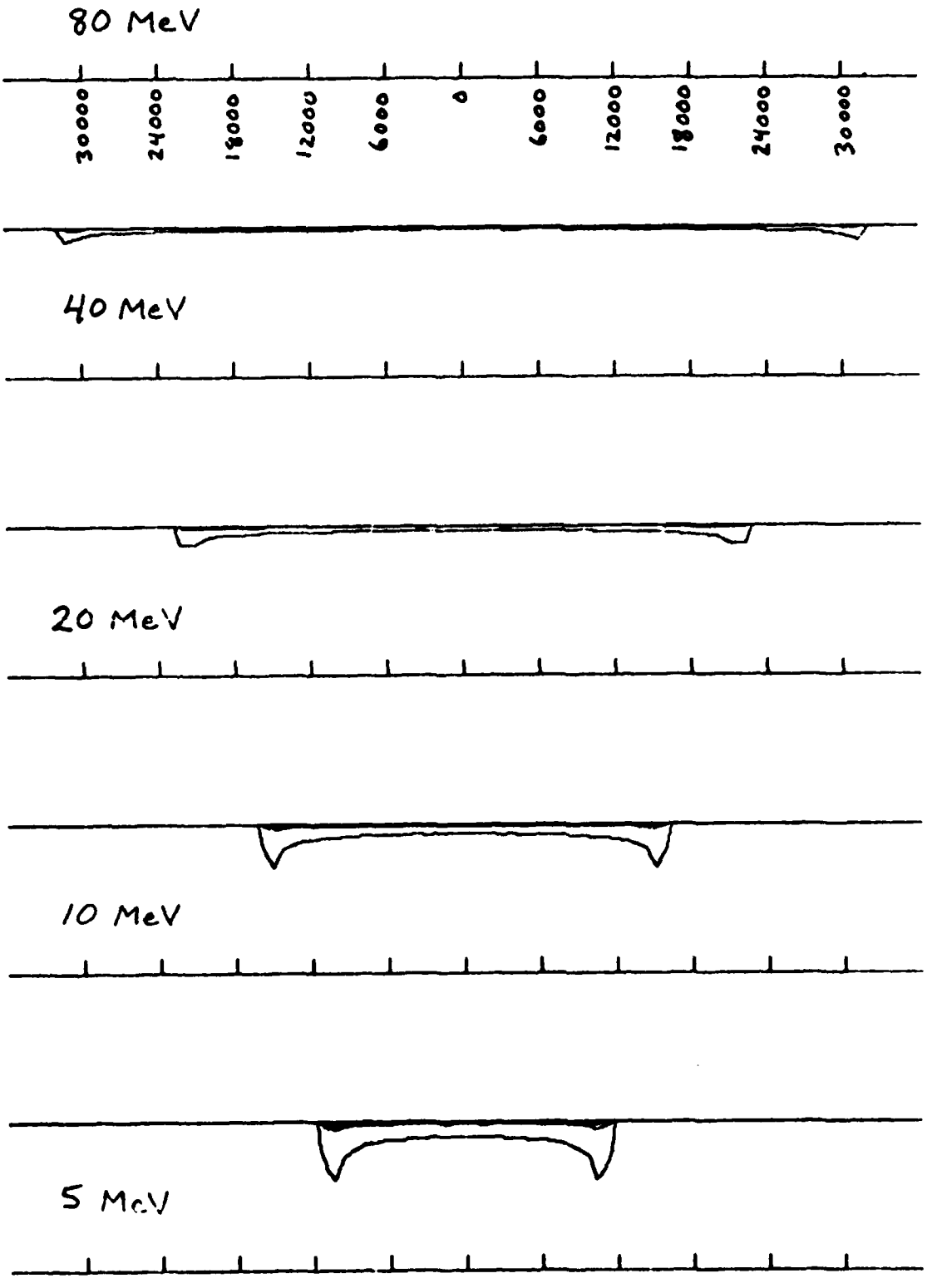

Acknowledgments

This work was supported by Ames Research Center/NASA contract NAS2-6553 and by the U. S. Office of Naval Research.

References

Cruikshank, D. P., Physical properties of the satellites of Saturn, in The Saturn System, edited by D. M. Hunten and D. Morrison, NASA Publication CP-2068, National Aeronautics and Space Administration, Washington, D. C., 1978.

Mead, G. D. and W. N. Hess, Jupiter's radiation belts and the sweeping effects of its satellites, J. Geophys. Res. 78, 2793, 1973.

Schultz, M. and L. J. Lanzerotti, Particle Diffusion in the Radiation Belts, Springer-Verlag, Berlin, 1974.

Thomsen, M. F., On determining a radial diffusion coefficient from the observed effects of Jupiter's satellites, Ph. D. thesis, University of Iowa, Iowa City, 1977.

Thomsen, M. F., Jovian magnetosphere-satellite interactions: Aspects of energetic charged particle loss, Rev. Geophys. and Space Phys., 17, 369, 1979.

Thomsen, M. F. and J. A. Van Allen, Motion of trapped electrons and protons in Saturn's inner magnetosphere, J. Geophys. Res. 85, (in press), 1980.

Van Allen, J. A., M. F. Thomsen, B. A. Randall, R. L. Rairden, and C. L. Grosskreutz, Saturn's magnetosphere, rings, and inner satellites, Science, 207, 415, 1980a.

Van Allen, J. A., M. F. Thomsen, and B. A. Randall, The energetic charged particle absorption signature of Mimas, J. Geophys. Res., 85, (in press), 1980b.